

## Metamagnetic behavior of fcc iron

Genrich L. Krasko

*Department of Materials Science and Engineering, Massachusetts Institute of Technology, Cambridge, Massachusetts 02139*

(Received 11 May 1987)

The Stoner model of itinerant ferromagnetism in combination with self-consistent linear muffin-tin orbital non-spin-polarized calculations are used for analysis of metamagnetic behavior of fcc iron. The developed procedure enables one to identify all the possible ferromagnetic phases (stable, metastable, and unstable) and find the areas of their existence. The results obtained earlier by Moruzzi and co-workers using the fixed spin-moment method are confirmed. Moreover, it is found that fcc iron has three (rather than two) different ferromagnetic states stable at the same volume: the high-spin (HS) state and two low-spin (LS1 and LS2) states. The LS states exist in the narrow areas within the range of stability of the HS state (rather than outside). The border of stability of the nonmagnetic phase is also found, and the theoretical explanation of two types of metamagnetic behavior observed earlier is suggested.

A hypothesis that fcc iron may exist in two different magnetic states was first put forward twenty-five years ago to explain the observed thermodynamics of fcc-bcc phase transformation in steels.<sup>1,2</sup> It was argued that one of the states was antiferromagnetic with a moment of  $0.5 \mu_B$ /atom, while the other state was ferromagnetic with a moment of  $2.8 \mu_B$ /atom. A two-level model was then explored in a quantitative thermodynamic analysis.

However, for some time there has been neither direct experimental nor theoretical confirmation of this hypothesis. In the late 1970's, it was shown<sup>3-5</sup> that the canonical-band theory<sup>6</sup> in combination with the Stoner model of itinerant ferromagnetism<sup>7</sup> did predict the existence of two ferromagnetic states in fcc iron. This approach also resulted in a simple and physically transparent explanation of ferromagnetism in transition metals and its trends throughout the periodic table, in terms of the density of states (DOS) of nonmagnetic systems. The idea was further developed in<sup>8,9</sup> using the hybridized DOS to confirm the existence of two magnetic states in fcc iron.

In recent years iron has been an object of extensive study by various efficient first-principles methods of band-structure and total-energy calculations (see, e.g., Refs. 10 and 15). In this paper we shall not be discussing the difficulties<sup>11,12</sup> in correctly predicting the energetics of different crystallographic modifications of iron which are believed to originate from the local spin-density approximation. Rather, we shall focus on the iron magnetic behavior.

Kuebler<sup>13</sup> was the first to report the results of self-consistent spin-polarized calculations, which confirmed the existence of two ferromagnetic states in fcc iron: a low-spin (LS) state with the magnetic moment,  $m$ , less than  $0.6\mu_B$ , and a high-spin (HS) state with  $m > 2\mu_B$  separated by discontinuity in the moment versus Wigner-Seitz radius dependence. Similar results were later reported in Refs. 12 and 14.

However, in recent papers,<sup>15</sup> a somewhat different be-

havior of ferromagnetic fcc iron has been discovered. There, a new "fixed spin-moment method" was used which allowed one to find the ground-state energy of a constrained system, with a fixed volume (or a Wigner-Seitz radius,  $s$ ) and a fixed magnetic moment per atom,  $m$ . The analysis of binding surfaces in the two-parameter ( $s, m$ ) space demonstrates a metamagnetic behavior of fcc iron: In an interval of  $s$ , both nonmagnetic and ferromagnetic phases are stable. Moreover, the LS state exists in a narrow area within the range of stability of the HS state, rather than outside this range, as previously believed.<sup>3-5,9,12,13</sup>

In the present paper we show that the Stoner approach in combination with self-consistent non-spin-polarized linear muffin-tin orbital (LMTO) calculations enables one to perform the detailed analysis of ferromag-

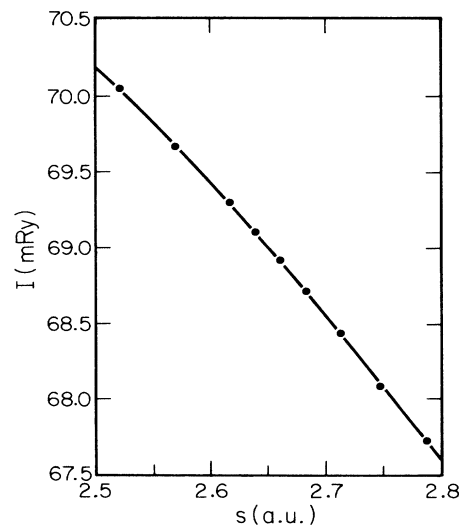


FIG. 1. The Stoner exchange parameter,  $I = 1.075I_0$ , as a function of the Wigner-Seitz radius,  $s$ .

TABLE I. Dependence of magnetic moment ( $\mu_B/\text{atom}$ ) and magnetic energy (mRy) on Stoner parameter (mRy).

$S$ (a.u.)	$I_0$	$\beta=1.000$		$\beta=1.025$		$\beta=1.050$		$\beta=1.075$		Our spin-polarized calculations	
		$m$	$E_m$	$m$	$E_m$	$m$	$E_m$	$m$	$E_m$	$m_d$	$m_{\text{tot}}$
2.6830	63.920	no solution		2.505	+ 3.693	2.520	+ 1.152	2.559	- 1.450	2.556	2.494
2.7125	63.668	2.554	+ 1.337	2.571	- 1.268	2.589	- 3.918	2.607	- 6.611	2.603	2.536

netic behavior, identify all the possible magnetic phases, both stable, metastable, and unstable, and find the areas of their emergence. Such an analysis, using traditional spin-polarized calculations, is at present either too cumbersome and expensive or even impossible, especially if a metastable energy minimum is too shallow or stationary unstable states are of interest. We confirm results of Ref. 15; we also show that fcc iron happens to have three (rather than two) different stable ferromagnetic states which may, in principle, coexist in a constant volume regime.

The Stoner model, in its original formulation, postulates that the change of energy upon forming a ferromagnetic state with moment  $m$  consists of two parts. The exchange energy contribution is simply  $-\frac{1}{4}Im^2$ , where  $I$  is the so-called Stoner exchange parameter, a constant. The kinetic energy term is found by forming two sub-bands for spin-up and spin-down electrons by flipping  $m/2$  spin-down  $d$  electrons from just below the nonmagnetic Fermi level into the nonoccupied spin-up states just above the Fermi level. As previously shown<sup>5,6,16-18</sup> this procedure corresponds to the first-order perturbation theory in  $m/n_d$  ( $n_d$  is the number of  $d$  electrons per atom). Thus, for a given (even constrained)  $m$ ,

$$E_m = \frac{1}{2} \int_0^m \frac{m' dm'}{\bar{N}(m', s)} - \frac{1}{4} Im^2, \quad (1)$$

where  $\bar{N}(m, s)$  is the nonmagnetic DOS averaged be-

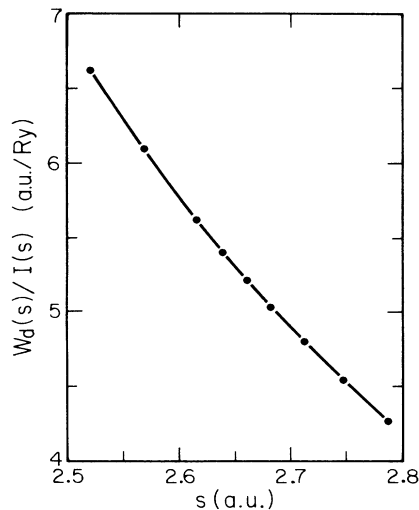


FIG. 2. The right-hand side of Eq. (8),  $W_d(s)/I(s)$ , as a function of the Wigner-Seitz radius,  $s$ .

tween the Fermi levels of spin-up and spin-down  $d$  electrons as found from the rigid sub-band shift. The procedure of “constructing”  $\bar{N}(m, s)$  is described elsewhere (see, e.g., Ref. 6).

The requirement of stationarity of  $E_m$ ,

$$\partial E_m / \partial m = 0, \quad (2)$$

gives, apart from the “trivial” solution,  $m = 0$ , the criterion of forming a ferromagnetic state:

$$I \bar{N}(m, s) = 1. \quad (3)$$

Let Eq. (3) have a solution,  $m$ . Then, the corresponding ferromagnetic state is stable ( $\partial^2 E_m / \partial m^2 > 0$ ) if

$$\partial \bar{N}(m, s) / \partial m < 0, \quad (4)$$

otherwise, it is unstable ( $\partial^2 E_m / \partial m^2 < 0$ ).

However, even if Eq. (3) holds, the ferromagnetic transition may not occur if  $E_m > 0$ . In this case the ferromagnetic state is metastable.

As for the nonmagnetic state,  $m = 0$ , it is stable and may coexist with a ferromagnetic state only so far as

$$(\partial^2 E_m / \partial m^2)_{m=0} \geq 0, \quad (5)$$

or, equivalently,

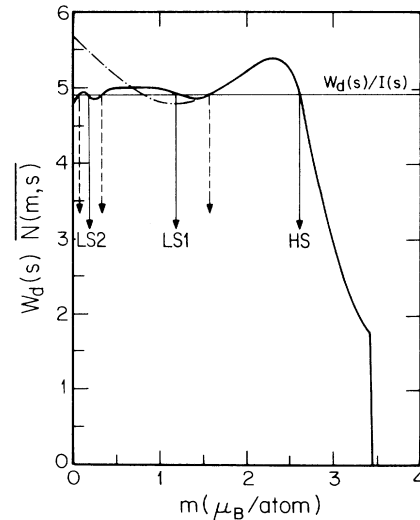


FIG. 3. Solving Eq. (8): The intersections of the left-hand side,  $W_d(s)\bar{N}(m, s)$  (almost independent of  $s$ ) with the right-hand side,  $W_d(s)/I(s)$ , for each  $s$  give all the possible stationary ferromagnetic solutions. The broken arrows show unstable solutions. The solutions shown correspond to  $s = 2.70$  a.u. For explanation of dot-dashed lines here and in Fig. 4, see the text.

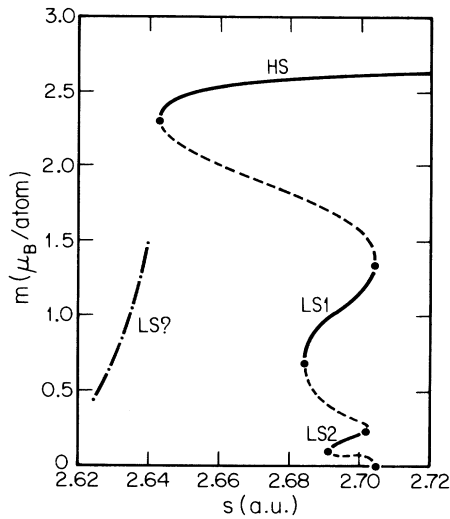


FIG. 4. Stationary magnetic moment as a function of the Wigner-Seitz radius. HS, LS1, and LS2 are the stable branches. The dashed-line branches are unstable. The non-magnetic state is stable along the  $s$  axis up to the point where the lowest unstable branch begins (2.706 a.u.).

$$IN(E_F) \leq 1, \quad (6)$$

where  $N(E_F) = \overline{N}(0, s)$  is the nonmagnetic  $d$  DOS at the Fermi level.

In the Stoner model,  $I$  may be thought of as an adjustable parameter. However, from the perturbation-theory analysis,<sup>5,6,16-18</sup>  $I$  can be found in terms of a nonmagnetic system. From the linear response theory<sup>18</sup> it follows that

$$I = \int d^3r \gamma^2(r) |K(r)|, \quad (7)$$

$$\gamma(r) = \sum_i^{\text{occ}} \frac{\delta(E_F - E_i^d) |\psi_i^d(r)|^2}{N(E_F)},$$

$$K(r) = \frac{1}{2} \frac{\delta^2 E_{xc}[\rho, m]}{\delta m^2} \Big|_{m=0}.$$

Here  $E_i^d$  and  $\psi_i^d(r)$  are, respectively, the  $d$  eigenvalues and wave functions of the nonmagnetic system;  $E_{xc}[\rho, m]$  is the exchange-correlation functional. In this case the Stoner model comprises a first-principles perturbation-theory approach which circumvents the iterative self-consistency scheme normally used to minimize the total energy with respect to the spin density.

In our calculations the LMTO method<sup>6,19,20</sup> with the so-called combined correction term<sup>6,20</sup> was used. The scalar-relativistic calculations for fcc iron on a uniform mesh of 946 points in the irreducible  $\frac{1}{48}$  wedge of the Brillouin zone were done, with the exchange-correlation functional of von Barth and Hedin.<sup>21</sup> Also, the frozen-core approximation was used.<sup>22</sup>

The Stoner parameter,  $I$ , was calculated from Eq. (7). It has been believed that  $I$  is essentially a constant, in-

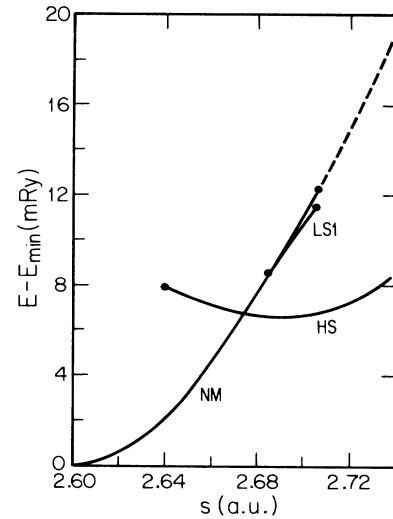


FIG. 5. Total energy vs  $s$  (c.f. Fig. 10 of Ref. 15). Both HS and LS1 phases have areas of metastability. The LS2 phase is not resolved in this energy scale (see Fig. 6). NM here refers to the nonmagnetic phase.

dependent of both the volume and crystallographic modification of the metal. The calculations revealed a monotonic dependence of  $I(s)$  (Fig. 1). Both the magnetic energy, Eq. (1), and the equilibrium moment,  $m$  [as found from Eq. (2)], happen to be rather sensitive to the values of  $I$ . In Table I we compare the  $m$ 's, found with  $I = \beta I_0$  [where  $I_0$  is the "first-principles" value, Eq. (7), and  $\beta = 1.0, 1.050, \text{ and } 1.075$ ] for two values of  $s$ , with those obtained in the spin-polarized calculations. One can see that for  $\beta = 1.075$  the calculated Stoner magnetic moments are almost equal to the  $d$ -electron components

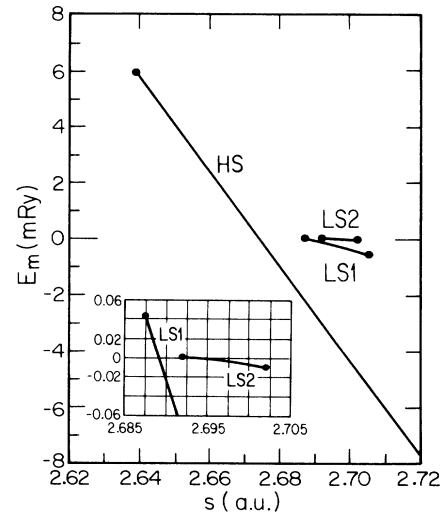


FIG. 6. Magnetic energy,  $E_m$ , of HS, LS1, and LS2 phases. Bold dots show the borders of stability.

TABLE II. Magnetic behavior of fcc iron in  $(s, m)$  plane.

	unstable NM	HS	stable LS1	LS2
Our work	$s \geq 2.706$	$s \geq 2.642$ $m \geq 2.40$	$2.704 \geq s \geq 2.687$ $1.40 \geq m \geq 0.75$	$2.705 \geq s \geq 2.691$ $0.23 \geq m \geq 0.14$
Ref. 15	$s \geq 2.685$	$s \geq 2.660$ $m \geq 2.40$	$2.685 \geq s \geq 2.670$ $1.50 \geq m \geq 0.90$	no solution

of the spin-polarized results. In order to be able to make quantitative comparison with the results of Ref. 15, we have chosen to perform the analysis for  $\beta=1.075$ .

As we mentioned above, the magnetic moments corresponding to the stationarity condition, Eq. (2), satisfy the Stoner equation, Eq. (3).  $\overline{N}(m, s)$  varies inversely as the width of the  $d$  band,  $W_d(s)$ . Therefore, for illustrative purposes, it is convenient to rewrite Eq. (3) in the form

$$W_d(s)\overline{N}(m, s) = \frac{W_d(s)}{I(s)}. \quad (8)$$

The left-hand side of this equation is almost independent of  $s$ , while the right-hand side decays with  $s$  (Fig. 2). Figure 3 illustrates solving Eq. (8). Intersections of curve  $W_d\overline{N}$  with horizontal lines  $W_d/I$  give for each  $s$  all the stationary solutions. For qualitative analysis, the  $W_d\overline{N}$  curve may be thought of as unchanging, while, with increasing  $s$ , the horizontal line, according to Fig. 2, goes down producing an  $m(s)$  plot. The loci of the curve with negative slope [Eq. (4)] generate stable solutions, while the positive slope loci give unstable solutions.

Figure 4 shows the  $m(s)$  plot for  $\beta=1.075$ . The dashed-line parts of the curve correspond to unstable ferromagnetic states. One can see that there exist three stable (one high spin and two low spin) branches: Preserving the existing terminology and abbreviations,

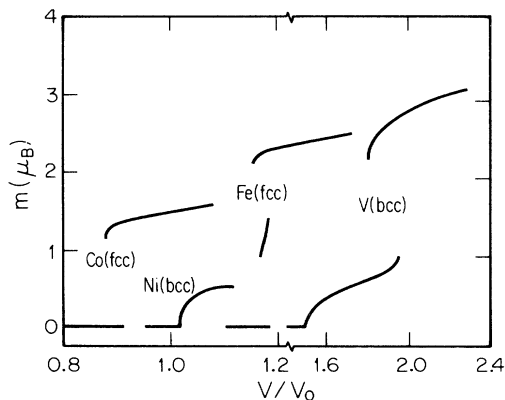


FIG. 7. Two types of metamagnetic behavior (Ref. 15). (i) The LS branch begins at the loss of stability point of the nonmagnetic state (Ni, V). (ii) A gap exists between the nonmagnetic and ferromagnetic solutions (Fe, Co).

we call them HS, LS1, and LS2. The nonmagnetic state is stable [Eqs. (5) and (6) hold] along the  $s$  axis up to the point where the lowest unstable branch begins ( $s=2.706$ ).

The energy plots of the nonmagnetic, and the three ferromagnetic states are shown in Figs. 5 and 6. The bold dots indicate the borders of stability of the corresponding magnetic states: For  $s < 2.642$  no magnetic (HS) solution exists; LS1 and LS2 exist, respectively, at  $2.687 < s < 2.704$  and  $2.691 < s < 2.705$ .<sup>23</sup> The three branches have areas of metastability ( $E_m > 0$  in Fig. 6). The nonmagnetic state becomes unstable along the broken line in Fig. 5.

The results of our analysis agree both qualitatively and quantitatively with the data obtained by the fixed spin-moment method and reported Ref. 15. We compare the two sets of data in Table II.

It was shown in Ref. 15 that two types of metamagnetic behavior are possible. As one can see in Fig. 7 (taken from Ref. 15), the lowest ferromagnetic branch may either (i) begin immediately from the point where the nonmagnetic phase loses stability (Ni, V) or (ii) after a gap in magnetic moment (Co, Fe). It follows from our analysis that the type of the behavior depends on whether the slope of  $\overline{N}(m, s)$  at  $m \rightarrow 0$  is positive or negative. From the Taylor expansion around  $E_F$ ,

$$\overline{N}(m, s) = N(E_F)(1 + \alpha m^2) \quad \text{when } m \rightarrow 0, \quad (9)$$

$$\alpha = \frac{1}{24} \left[ \frac{N''(E_F)}{N(E_F)^3} - \frac{3}{N(E_F)^2} \left( \frac{N'(E_F)}{N(E_F)} \right)^2 \right],$$

where  $N(E_F)$ ,  $N'(E_F)$ , and  $N''(E_F)$  are the nonmagnetic  $d$  DOS at  $E_F$  and its first and second derivatives.

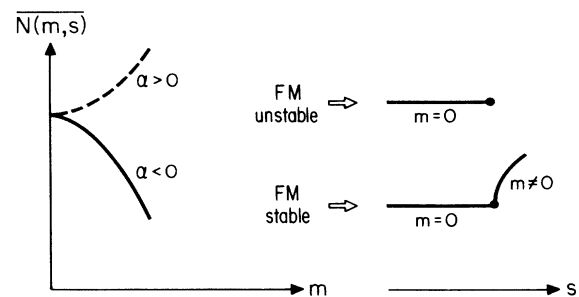


FIG. 8. Theoretical explanation of situations (i) and (ii) of Fig. 7. FM represents ferromagnetic.

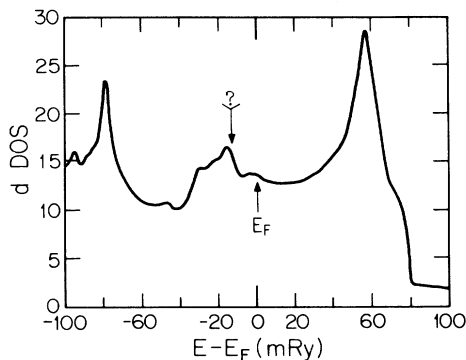


FIG. 9. The high-resolution  $d$  DOS for NM phase. See the explanation in the text.

Thus, case (i) is realized when  $\alpha < 0$ ; otherwise ( $\alpha > 0$ ), case (ii) takes place. This is illustrated in Fig. 8. It is obvious that, due to the complex shape of  $N(E)$ , *a priori* prediction of the type of metamagnetic behavior is virtually impossible.

Finally, in Fig. 9 the  $d$  DOS for nonmagnetic fcc iron is shown. One can see that the Fermi level,  $E_F$ , falls on the slope of the high-energy side of the tiny peak. In order to produce  $\bar{N}(m, s)$  of the dot-dash line of Fig. 3 and hence the magnetic behavior of the dot-dash line of Fig. 4,  $E_F$  would have to be shifted by about 15 mRy to

somewhere around the unmarked arrow. We, however, were unable to achieve such a shift by introducing “perturbations” into the computational procedure, such as increasing the number of points in the irreducible wedge of the Brillouin zone or the number of basis orbitals. We, therefore, believe that the observed behavior is meaningful and the results are reliable.

In conclusion, we would like to once again stress that the Stoner model in combination with reliable nonmagnetic calculations enables one to perform a simple and detailed analysis of ferromagnetic behavior. Such an analysis is at present very difficult or even impossible using the spin-polarized calculations. The Stoner approach also may be used as a preliminary analysis in a complex spin-polarized problem.

#### ACKNOWLEDGMENTS

The author expresses deep gratitude to Professor O. Andersen and the members of his group for the hospitality extended during the author’s stay at the Max-Planck-Institut für Festkörperforschung in Stuttgart, FRG, where part of the present work was done. Many fruitful discussions with O.-K. Andersen, N. Christensen, O. Gunnarsson, and O. Jepsen of MPI and G. Olson of MIT are gratefully acknowledged. In all the calculations, the LMTO computer code developed by N. Christensen has been used.

<sup>1</sup>K. G. Tauer and R. J. Weiss, *Bull. Am. Phys. Soc.* **6**, 125 (1961).

<sup>2</sup>L. Kaufman, E. V. Clougherty, and R. J. Weiss, *Acta Metall.* **11**, 323 (1963).

<sup>3</sup>J. Madsen, O. K. Andersen, U. K. Poulsen, and O. Jepsen, *Magnetism and Magnetic Materials, Philadelphia, 1975*, proceedings of the meeting of the American Physics Society, edited by Hugh C. Wolfe (AIP, New York, 1976).

<sup>4</sup>U. K. Poulsen, J. Kollar, and O. K. Andersen, *J. Phys. F* **6**, L241 (1976).

<sup>5</sup>O. K. Andersen, J. Madsen, U. K. Paulsen, O. Jepsen, and J. Kollar, *Physica* **86–88B**, 249 (1977).

<sup>6</sup>O. K. Andersen, O. Jepsen, and D. Gloetzel in *Highlights of Condensed Matter Theory*, edited by F. Bassani, F. Fumi, and M. P. Tosi (North-Holland, New York, 1985).

<sup>7</sup>E. C. Stoner, *Proc. R. Soc. London, Ser. A* **169**, 339 (1939).

<sup>8</sup>D. M. Roy and D. G. Pettifor, *J. Phys. F* **7**, 1183 (1977).

<sup>9</sup>D. G. Pettifor, *CALPHAD: Comput. Coupling Phase Diagrams Thermochem.* **1**, 305 (1977).

<sup>10</sup>K. B. Hathaway, H. J. F. Jansen, and A. J. Freeman, *Phys. Rev. B* **31**, 7603 (1985).

<sup>11</sup>H. J. F. Jansen, K. B. Hathaway, and A. J. Freeman, *Phys. Rev. B* **30**, 6177 (1984).

<sup>12</sup>C. S. Wang, B. M. Klein, and H. Krakauer, *Phys. Rev. Lett.* **54**, 1852 (1985).

<sup>13</sup>J. Kuebler, *Phys. Lett.* **81A**, 81 (1981).

<sup>14</sup>D. Bagayoko and J. Callaway, *Phys. Rev. B* **28**, 5419 (1983).

<sup>15</sup>V. L. Moruzzi, *Phys. Rev. Lett.* **57**, 2211 (1986); V. L. Moruzzi, P. M. Marcus, K. Schwarz, and P. Mohn, *Phys. Rev. B* **34**, 1784 (1986).

<sup>16</sup>S. H. Vosko and J. P. Perdew, *Can. J. Phys.* **53**, 1385 (1975).

<sup>17</sup>O. Gunnarsson, *J. Phys. F* **6**, 587 (1976).

<sup>18</sup>J. F. Janak, *Phys. Rev. B* **16**, 255 (1977).

<sup>19</sup>O. K. Andersen in *Electronic Structure of Complex Systems*, edited by P. Phariseau and W. M. Timmerman (Plenum, New York, 1984), p. 11–65.

<sup>20</sup>H. L. Skriver, *The LMTO Method* (Springer, Berlin, 1984).

<sup>21</sup>U. von Barth and L. Hedin, *J. Phys. C* **5**, 1629 (1972).

<sup>22</sup>U. von Barth and C. D. Gelatt, *Phys. Rev. B* **21**, 2222 (1980); see also discussion of the effect of  $3p$  core electrons on the structural energies in Ref. 10.

<sup>23</sup>It should be pointed out that although the solutions of Eq. (3) [or Eq. (8)] are sensitive to the values of  $I$ , the main features of the ferromagnetic “spectrum” are not. As one can see from Fig. 3, the possible solutions of Eq. (8) (intersections with the horizontal line  $W_d/I$ ) are, in fact, functions of  $W_d/I$ , rather than  $s$ . This means that an *ad hoc* change of  $I$  will simply change the  $s$  interval of metamagnetic solutions. The Wigner-Seitz radius  $s$  corresponding to each solution and the  $s$  interval of their coexistence will then scale as  $(I_0/I)^{1/5}$  since  $W_d$  scales as  $s^{-5}$ . Otherwise the spectrum of ferromagnetic solutions remains virtually unchanged. Drastic changes in this spectrum would arise only if the “wiggles” on  $\bar{N}(m, s)$  [or  $W_d\bar{N}(m, s)$ ] at small  $m$  could be deformed, smoothed out, or eliminated altogether. We have been unable to do that by introducing computational “perturbations” mentioned at the end of this paper.